MicroRNA-101, Down-regulated in Hepatocellular Carcinoma, Promotes Apoptosis and Suppresses Tumorigenicity

Hang Su,[1] Jian-Rong Yang,[1] Teng Xu,[1] Jun Huang,[2,3] Li Xu,[2,3] Yunfei Yuan,[2,3] and Shi-Mei Zhuang[1,2]

[1]Key Laboratory of Gene Engineering of the Ministry of Education, State Key Laboratory of Biocontrol, School of Life Sciences; [2]State Key Laboratory of Oncology in Southern China, Cancer Center; and [3]Department of Hepatobiliary Oncology, Cancer Center, Sun Yat-sen University, Guangzhou, P.R. China

Abstract

Although aberrant microRNA (miRNA) expressions have been observed in different types of cancer, their pathophysiologic role and their relevance to tumorigenesis are still largely unknown. In this study, we first evaluated the expression of 308 miRNAs in human hepatocellular carcinoma (HCC) and normal hepatic tissues and identified 29 differentially expressed miRNAs in HCC tissues. miR-101, a significantly down-regulated miRNA, was further studied in greater detail because the signal pathway(s) regulated by miR-101 and the role of miR-101 in tumorigenesis have not yet been elucidated. Interestingly, decreased expression of miR-101 was found in all six hepatoma cell lines examined and in as high as 94.1% of HCC tissues, compared with their nontumor counterparts. Furthermore, ectopic expression of miR-101 dramatically suppressed the ability of hepatoma cells to form colonies *in vitro* and to develop tumors in nude mice. We also found that miR-101 could sensitize hepatoma cell lines to both serum starvation– and chemotherapeutic drug–induced apoptosis. Further investigation revealed that miR-101 significantly repressed the expression of luciferase carrying the 3′-untranslated region of Mcl-1 and reduced the endogenous protein level of Mcl-1, whereas the miR-101 inhibitor obviously up-regulated Mcl-1 expression and inhibited cell apoptosis. Moreover, silencing of *Mcl-1* phenocopied the effect of miR-101 and forced expression of Mcl-1 could reverse the proapoptotic effect of miR-101. These results indicate that miR-101 may exert its proapoptotic function via targeting Mcl-1. Taken together, our data suggest an important role of miR-101 in the molecular etiology of cancer and implicate the potential application of miR-101 in cancer therapy. [Cancer Res 2009;69(3):1135–42]

Introduction

MicroRNAs (miRNA) belong to a class of endogenously expressed, noncoding small RNAs, which contain ~22 nucleotides. It has been shown that miRNAs can regulate the expression of protein-coding genes at the posttranscriptional level through imperfect base pairing with the 3′-untranslated region (3′-UTR) of target mRNAs (1). Growing evidence suggests that deregulation of miRNAs may contribute to many types of human diseases, including cancer. It has been shown that 50% of miRNAs are located within the chromosomal regions known to be frequently amplified or deleted in human cancer cells (2). Furthermore, misexpression of miRNAs has been observed in various types of cancers (3, 4) and is also associated with the clinical outcome of cancer patients (5, 6). Even more, the expression profiles of miRNAs give much more accurate classification on the tissue origin of poorly differentiated cancer cells, compared with that of mRNA (3). Consistently, miRNAs have been implicated in the regulation of various cellular processes that are often deregulated during tumorigenesis (1, 7–9). These data highlight the importance of miRNAs in cancer development and provide new insights into the molecular mechanisms underlying tumorigenesis.

Hepatocellular carcinoma (HCC) is one of the most common cancers worldwide and among the leading causes of cancer-related death (10). Like other cancers, the development of HCC is a multistep process with accumulation of genetic and epigenetic changes (11, 12). Altered miRNA expressions have been observed in HCCs that originated from different geographic areas (5, 8, 13–18). Furthermore, several miRNAs deregulated in HCC, such as miR-21, miR-221, miR-223, and miR-224, have been identified as modulators of cell growth, apoptosis, migration, or invasion (8, 16, 18, 19). These findings suggest the involvement of miRNAs in the pathogenesis of HCC. Obviously, more extensive investigations on the functions of miRNAs that are deregulated in HCC are required to elucidate the role of miRNAs in hepatocarcinogenesis.

In this study, the expression profiles of 308 miRNAs were examined in human HCC and normal hepatic tissues. Moreover, a set of significantly differentially expressed miRNAs were identified in HCC tissues. Further investigation revealed that a frequently down-regulated miRNA, miR-101, could sensitize tumor cells to apoptosis and impaired the ability of cancer cells to form colony *in vitro* and to develop tumor *in vivo*. Moreover, myeloid cell leukemia sequence 1 (Mcl-1), an antiapoptotic member of Bcl-2 family, was characterized as a direct target of miR-101. Our findings will help to elucidate the functions of miRNAs and their roles in tumorigenesis.

Materials and Methods

Tissue specimens and cell lines. Normal liver tissues were collected from patients undergoing resection of hepatic hemangiomas. Paired HCC and adjacent nontumor liver tissues were obtained from patients undergoing resection of HCC. No previous local or systemic treatment had been conducted for these patients before operation. The specimens were collected between 2005 and 2006 at the Cancer Center, Sun Yat-sen University, Guangzhou, P.R. China. Tissue samples were immediately snap frozen in liquid nitrogen until use. Both tumor and noncancerous samples

Note: Supplementary data for this article are available at Cancer Research Online (http://cancerres.aacrjournals.org/).

Requests for reprints: Shi-Mei Zhuang, Key Laboratory of Gene Engineering of the Ministry of Education, School of Life Sciences, Sun Yat-sen University, 135 Xingangxi Road, Guangzhou 510275, P.R. China. Phone: 86-20-84112164; Fax: 86-20-84112169; E-mail: LSSZSM@mail.sysu.edu.cn or zhuangshimei@163.com and Yunfei Yuan, Department of Hepatobiliary Oncology, Cancer Center, Sun Yat-sen University, 651 Dongfengdong Road, Guangzhou 510060, P.R. China. Phone: 86-20-87343118; Fax: 86-20-87343392; E-mail: yuanyf@mail.sysu.edu.cn.

doi:10.1158/0008-5472.CAN-08-2886

were histologically confirmed. All patients were unrelated ethnic Han Chinese who lived in Southeast China. Hepatitis B virus (HBV) or hepatitis C virus (HCV) infection was diagnosed when HBV surface antigen (HBsAg) or HCV antibody was detected by ELISA in the serum isolated from peripheral blood. HBV infections were identified in two of three patients with hepatic hemangiomas and in 90.9% of HCC cases, whereas none of the HCV infection was found in these patients. All HCC tumors were originated from the background of chronic hepatitis or cirrhosis. Informed consent was obtained from each patient. This study was approved by the Institute Research Ethics Committee at Cancer Center, Sun Yat-sen University.

The cell lines used in this study included immortalized mouse embryonic fibroblast cell line NIH/3T3, SV40-transformed embryonic kidney cell line 293T, cervical cancer cell line HeLa, immortalized liver cell line L-02, and six human liver cancer cell lines (HepG2, Hep3B, SK-Hep1, Huh7, QGY-7703, and SMMC-7721). They were all maintained in DMEM (Hyclone) supplemented with 10% fetal bovine serum (FBS, PAA Laboratories GmbH).

Microarray. Total RNAs, isolated from five HCCs and three normal liver tissues using Trizol reagent (Invitrogen), were sent to CapitalBio Corp. for noncoding RNA microarray analysis. The microarray analysis was done as described on the Web site of CapitalBio.[4] Briefly, ~60 μg of total RNAs were used to extract small-sized RNA using miRNA Isolation Kit (Ambion, Inc.). Fluorescein-labeled miRNAs were hybridized to each noncoding RNA microarray slide, which contains probes complementary to 308 human miRNAs registered in miRBase 11.0.[5] Each probe was spotted in triplicate in each slide and every sample was assayed in duplicate. The microarray platform and data have been submitted to the Gene Expression Omnibus public database[6] at the National Center for Biotechnology Information, following the Minimum Information About a Microarray Gene Experiment guidelines. The accession numbers are GPL7274 (platform) and GSE12717 (samples; release date September 2008). To allow the comparison among different slides, the signal intensity from each spot was log transformed and normalized using the quantile normalization method in the Bioconductor package,[7] as described previously (20). Therefore, the expression level of each miRNA in every sample was represented by the mean of normalized log-transformed values from the duplicate slides. To lessen the effect of random fluctuation on the significance of expression difference, only those miRNAs that displayed signal intensity higher than 1,000 in at least one of the eight examined samples were applied to the statistical comparison between the normal and HCC tissues. This comparison was done with Significance Analysis of Microarrays in the Bioconductor package.

Northern blot. Small-sized RNAs were enriched from total RNAs using PEG8000 as described previously (21). Briefly, 100 to 200 μg of total RNAs in a volume of 600 μL were mixed with 75 μL each of 50% PEG8000 and 5 mol/L NaCl, followed by incubation on ice for 2 h and centrifugation at 12,000 × *g* for 10 min. The supernatant was collected, mixed with 1/10 volume of 3 mol/L sodium acetate and 4 volumes of cold absolute ethanol, incubated at −20°C overnight and then centrifuged at 24,000 × *g* for 1 h. The RNA pellet was washed with 80% ethanol, dried briefly, and resuspended in RNase-free water.

The expression level of miRNAs was examined by Northern blot, as described previously (22). The DNA oligonucleotide probes used to detect miR-101 and U6 snRNA were as follows: miR-101-5′-CTTCAGTTATCACAGTACTGTA and U6-5′-AACGCTTCACGAATTTGCGT. The band intensity was quantified using GeneTools software (version 3.03; SynGene).

RNA oligoribonucleotides and cell transfections. miR-101 mimic was a RNA duplex (Supplementary Fig. S1) designed as described previously (23). The small interference RNA (siRNA) targeting human Mcl-1 mRNA (Genbank accession no. NM_021960) was designated as siMCL1 (Supplementary Fig. S1). The control RNA duplex (named as NC) for both miRNA mimic and siRNA was nonhomologous to any human genome sequences (Supplementary Fig. S1). For *in vivo* tumorigenicity assay, all pyrimidine nucleotides in the NC or miR-101 duplex were substituted by their 2′-*O*-methyl analogues to improve RNA stability. The anti–miR-101, with sequence of 5′-CUUCAGUUAUCACAGUACUGUA, was a 2′-*O*-methyl–modified oligoribonucleotide designed as an inhibitor of miR-101. The anti–miR-C, with a sequence of 5′-GUGGAUAUUGUUGCCAUCA, was used as a negative control for anti–miR-101 in the antagonism experiment. All the RNA oligoribonucleotide(s) were purchased from Genepharma.

Reverse transfection of RNA oligoribonucleotide(s) was done using Lipofectamine RNAiMAX (Invitrogen) according to the manufacturer's protocol. The transfection efficiency, examined by a FAM-conjugated siRNA and fluorescence-activated cell sorting analysis, was ~77% in HepG2 cells (data not shown). Fifty nanomoles per liter of RNA duplex and 200 nmol/L of miRNA inhibitor were used for each transfection, unless otherwise indicated. In the rescue experiment, 24 h after RNA transfection, cells were transfected with 200 ng plasmids in a 24-well plate, using Lipofectamine 2000 (Invitrogen).

Colony formation assay. Twenty-four hours after transfection, 200 transfected cells were placed in a fresh six-well plate and maintained in DMEM containing 10% FBS for 2 wk. Colonies were fixed with methanol and stained with 0.1% crystal violet in 20% methanol for 15 min.

Tumorigenicity assays in nude mice. All experimental procedures involving animals were in accordance with the Guide for the Care and Use of Laboratory Animals (NIH publication nos. 80-23, revised 1996) and were performed according to the institutional ethical guidelines for animal experiment. miR-101– and NC-transfected HepG2 cells (5×10^4 or 1×10^5) were suspended in 100 μL PBS and then injected s.c. into either side of the posterior flank of the same female BALB/c athymic nude mouse at 5 to 6 wk of age. Tumor growth was examined daily for at least 5 wk. Tumor volume (V) was monitored by measuring the length (L) and width (W) with calipers and calculated with the formula ($L \times W^2$) × 0.5.

Vector construction. pGL3cm was created based on the firefly luciferase expressing vector pGL3-control (Promega) by creating *Bst*XI, *Eco*RI, *Eco*RV, and *Apa*I sites immediately upstream of the *Xba*I site, which was right downstream of the stop codon of the firefly luciferase reporter gene in pGL3-control.

To construct pGL3cm-MCL1-3′-UTR-WT plasmid, a wild-type 3′-UTR segment of human Mcl-1 mRNA (1208-1689 nt, Genbank accession no. NM_021960) containing the putative miR-101 binding sequence (1547–1568 nt) was amplified and cloned into the *Apa*I and *Xba*I sites downstream of the luciferase reporter gene in pGL3cm. pGL3cm-MCL1-3′-UTR-MUT, which carried the mutated sequence in the complementary site for the seed region of miR-101, was generated based on pGL3cm-MCL1-3′-UTR-WT plasmid by site-specific mutagenesis.

To construct the miR-101 expression vector (pc3-miR-101), a fragment encompassing the mature miR-101 sequence and its 5′- and 3′-flanking regions (213 and 362 bp, respectively) was amplified and then cloned into the *Bam*HI and *Eco*RI sites in pcDNA3.0 (Invitrogen).

The plasmid pc3-gab was produced based on pcDNA3.0 by replacing the *neomycin* open reading frame with an expression cassette of *enhanced green fluorescent protein* (*EGFP*) gene between the *Asu*II and *Bse*JI sites. The Mcl-1 expression vector (pc3-gab-MCL1) was created by cloning the *Mcl-1* coding sequence into the *Bam*HI and *Eco*RI sites of pc3-gab.

Luciferase reporter assay. For luciferase reporter assay, 293T cells (6×10^4) were plated in a 48-well plate and then cotransfected with 400 ng of either pc3-miR-101 or pcDNA3.0, 20 ng of either pGL3cm-MCL1-3′-UTR-WT or pGL3cm-MCL1-3′-UTR-MUT, and 4 ng of pRL-TK (Promega), using calcium phosphate precipitation. Cells were collected 48 h after transfection and analyzed using the Dual-Luciferase Reporter Assay System (Promega). Luciferase activity was detected by M200 microplate fluorescence reader (Tecan). The pRL-TK vector that provided the constitutive expression of *Renilla* luciferase was cotransfected as an internal control to correct the differences in both transfection and harvest efficiencies. Transfections were done in duplicates and repeated at least thrice in independent experiments.

[4] http://www.capitalbio.com
[5] http://microrna.sanger.ac.uk/sequences/
[6] http://www.ncbi.nlm.nih.gov/projects/geo/query/acc.cgi?acc=GSE12717
[7] http://www.bioconductor.org

Western blot. Cell protein lysates were separated in 10% SDS-polyacrylamide gels, electrophoretically transferred to polyvinylidene difluoride membranes (Roche), then detected with rabbit polyclonal antibody specific for Mcl-1 (Santa Cruz Biotechnology) and commercial ECL kit (Pierce). Protein loading was estimated using mouse anti–β-actin monoclonal antibody (Boster). The intensity of protein fragments was quantified using GeneTools software (version 3.03; SynGene).

Semiquantitative reverse transcription-PCR. To obtain cDNA, 2 μg of total RNAs were reverse transcribed using Moloney murine leukemia virus reverse transcriptase (Promega). Specific primers used for PCR amplification were as follows: 5′-AAGATGACCCAGATCATGTTTGAG and 5′-GCAGCTCGTAGCTCTTCTCCAG for β-actin, and 5′-AGAAAGCTGCATC-GAACCAT and 5′-CCAGCTCCTACTCCAGCAAC for Mcl-1. PCR products were then separated on 1.5% agarose gels containing ethidium bromide and visualized under UV trans-illumination. Quantification of each product was done using GeneTools software (version 3.03; SynGene).

Table 1. Summary of significantly differentially expressed miRNAs in HCC compared with normal liver tissues

miRNA	*P**	Fold change†	Chromosome location
Decreased expression			
miR-29c	0.007	0.174	1q32.2
miR-99a	0.024	0.219	21q21.1
miR-100	0.022	0.209	11q24.1
miR-101	0.009	0.214	1p31.3
			9p24.1
miR-125b	0.010	0.153	11q24.1
			21q21.1
miR-195	0.015	0.202	17p13.1
miR-199a-5p	0.014	0.149	1q24.3
			19p13.2
miR-199b-3p	0.009	0.112	9q34.11
miR-215	0.018	0.093	1q41
miR-223	0.029	0.267	Xq12
miR-365	0.007	0.127	16p13.12
miR-378	0.002	0.139	5q33.1
miR-422a	0.005	0.166	15q22.31
miR-424	0.001	0.092	Xq26.3
miR-520c-3p	0.036	0.218	19q13.41
Increased expression			
miR-18a	0.039	3.223	13q31.3
miR-18b	0.016	4.077	Xq26.2
miR-25	0.045	3.230	7q22.1
miR-93	0.024	4.111	7q22.1
miR-127-3p	0.014	6.770	14q32.31
miR-210	0.040	3.785	11p15.5
miR-216a	0.012	6.428	2p16.1
miR-222	0.011	4.964	Xp11.3
miR-224	<0.001	27.231	Xq28
miR-362-5p	0.016	3.902	Xp11.23
miR-382	0.020	5.661	14q32.31
miR-491-5p	0.011	5.222	9p21.3
miR-519b-5p	0.016	6.865	19q13.41
miR-527	0.026	5.745	19q13.41

*P values were calculated using Significance Analysis of Microarrays in the Bioconductor package (details in Materials and Methods). P value <0.05 was considered statistically significant.
†Only those miRNAs whose expression levels displayed >0.5-fold decrease or 2-fold increase in HCC tissues were listed.

Apoptosis assay. Apoptosis was evaluated by the apoptotic morphology, the activity of caspase-3/7, and the cell viability. For morphologic examination, cells were stained with 4,6-diamidino-2-phenylindole (DAPI; Sigma-Aldrich) and those with fragmented or condensed nuclei were counted as apoptotic cells. At least 500 cells were counted for each sample.

The activity of caspase-3 and caspase-7 was detected in 96-well format using the Caspase-Glo 3/7 Assay (Promega). One hundred microliters of the Caspase-Glo 3/7 reagent were added to each well and then incubated at room temperature for 1 h. The luminescence was detected using the M200 microplate fluorescence reader (Tecan). The background luminescence associated with cell culture and assay reagent (blank reaction) was subtracted from experimental value.

Cell viability was determined by the Alamar blue assay (AbD Serotec). Briefly, cells were transfected in a 24-well plate and replated into a 96-well plate at 10% confluency 24 h later, followed by the Alamar blue assay at indicated times. Fluorescence of the reduced Alamar blue dye was measured using M200 microplate fluorescence reader (Tecan) at excitation wavelength of 540 nm and emission wavelength of 590 nm.

Statistical analysis. Data are presented as mean ± SEM from at least three separate experiments. Multiple group comparisons were performed using ANOVA with a post hoc test for subsequent individual group comparisons. Differences were considered statistically significant at $P < 0.05$.

Results

miRNAs are differentially expressed in human HCC tissues. We first compared the miRNA expression profiles of three normal liver and five primary HCC samples. Among 308 human miRNAs analyzed, 29 of them exhibited significantly differential expression in HCC tissues (Table 1). The relative expression of these miRNAs is presented as a Heat Map in Supplementary Fig. S2. Among the 15 miRNAs that displayed decreased expression in HCC, miR-101 attracted our attention. The miR-101 coding genes, *MIRN101-1* and *MIRN101-2*, are located in the genomic loci with high frequency of allelic losses in several type of cancers (24, 25), including HCC (~40%; ref. 26). In addition, down-regulation of miR-101 has been observed in HCC (5) and cancers originated from lung (27), breast (28), cervix (29), and ovary (30), suggesting that deregulation of miR-101 may be involved in tumorigenesis. However, the signal pathway(s) regulated by miR-101 and the role of miR-101 in tumorigenesis are still largely unknown. Therefore, miR-101 was chosen for further study in greater detail.

Expression of miR-101 is frequently reduced in human HCC tissues and hepatoma cell lines. First, Northern blot analysis was performed to analyze the expression level of miR-101 in mouse and human normal liver tissues, and in cell lines including NIH/3T3, 293T, HeLa, L-02, as well as six human liver cancer cell lines (HepG2, Hep3B, SK-Hep1, Huh7, QGY-7703 and SMMC-7721). The mature form of miR-101 was readily detectable in both SV40-transformed 293T and immortalized NIH/3T3 cells (Fig. 1*A, lanes 6* and *7*), but at an obvious lower level compared with that in mouse and human normal liver tissues (Fig. 1*A, lanes 1* and *12*). In marked contrast, significant reduction in the expression of miR-101 was observed in L-02 and all cancer cell lines examined (Fig. 1*A*).

The expression level of miR-101 was further examined in 17 paired HCC and adjacent nontumor liver tissues. In comparison with the adjacent noncancerous tissues, miR-101 was down-regulated in all tumor samples except case 631 (94.1%; Fig. 1*B*). Furthermore, 13 of 17 (76.5%) HCC tissues revealed >50% reduction in the miR-101 level, relative to the corresponding nontumor

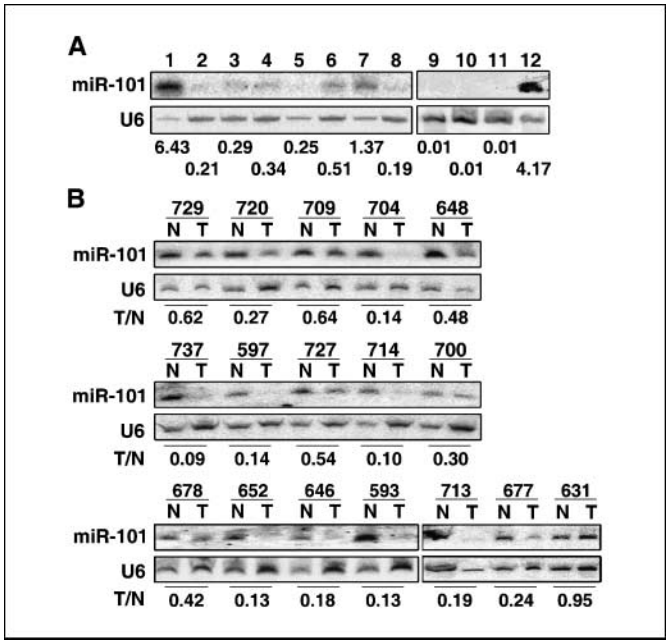

Figure 1. Analysis of miR-101 expression in cancer cell lines and human HCC tissues by Northern blot. *A,* expression level of miR-101 in normal liver tissues and various cell lines. *Lane 1,* normal murine liver tissue; *lane 2,* Huh7; *lane 3,* Hep3B; *lane 4,* HepG2; *lane 5,* SK-Hep1; *lane 6,* 293T; *lane 7,* NIH/3T3; *lane 8,* HeLa; *lane 9,* QGY-7703; *lane 10,* SMMC-7721; *lane 11,* L-02; *lane 12,* normal human liver tissue. *B,* expression level of miR-101 in 17 paired HCCs and adjacent nontumor tissues. *T,* HCC tissue; *N,* adjacent noncancerous liver tissue. The same membrane was hybridized sequentially with miR-101 and U6 probe, as indicated on the left. U6 was used as a control for RNA loading. The intensity for each band was densitometrically quantified. The value under each lane in *A* indicates the relative expression level of miR-101, which is represented by the intensity ratio between miR-101 and U6 fragments in each lane. The value under each pair of samples in *B* indicates the fold change of relative miR-101 expression level in HCC tissue, relative to that in adjacent nontumor tissue.

samples. These results suggest that reduced miR-101 expression is a frequent event in human HCC tissues and maybe involved in hepatocarcinogenesis.

miR-101 suppresses colony formation *in vitro* and tumorigenicity *in vivo*. The significant reduction of miR-101 expression in HCC samples prompted us to explore the possible biological significance of miR-101 in tumorigenesis. As an initial step, the capacity of colony formation was evaluated on liver cancer cell lines (HepG2 and QGY-7703) as well as cervical cancer cell line (HeLa) that were transfected with control RNA duplex (NC), miR-101 duplex, or without any transfection. Interestingly, miR-101–transfected cells displayed much fewer and smaller colonies compared with NC transfectants and nontransfected cells (Fig. 2*A*). These data indicate a growth-inhibitory role of miR-101.

To further confirm the above findings, an *in vivo* model was used. NC- and miR-101–transfected HepG2 cells were injected s.c. into either posterior flank of the same nude mice, respectively. In the first experimental group, 5×10^4 cells were injected and four nude mice were included. Five weeks after injection, no tumors were observed in the flanks injected with miR-101–transfected HepG2 cells. In sharp contrast, tumors appeared in the sites injected with NC transfectants in 3 of 4 (75%) mice. The tumor became palpable 24 to 29 days after inoculation and grew to 36 to 155 mm^3 at the end of observation (35 days). These results were reproducible when a larger number of cells (1×10^5) were injected into another five nude mice. Consistently, miR-101–transfected HepG2 cells did not produce any tumors 5 weeks after injection, whereas NC transfectants produced tumors (mean size of 584 ± 187 mm^3 at the end of observation) in 4 of 5 (80%) mice (Fig. 2*B*) 17 to 20 days after inoculation. These results indicate that introduction of miR-101 significantly inhibits tumorigenicity of HepG2 cells in nude mouse xenograft model.

Mcl-1 is a direct target of miR-101. The inhibitory role of miR-101 in tumorigenicity indicates that miR-101 may promote cell apoptosis and/or inhibit cell proliferation. It is generally accepted that miRNAs exert their function through regulating the expression of their downstream target gene(s). Thus, putative miR-101 targets were predicted using target prediction programs, TargetScan and miRanda. Our analysis revealed that Mcl-1, an antiapoptotic member of Bcl-2 family, was a potential target of miR-101. The 3′-UTR of Mcl-1 mRNA contained a complementary site for the seed region of miR-101 (Fig. 3*A*). In addition, Mcl-1 had been shown to be up-regulated in different cancer cells (31, 32) and to protect cells from various stimuli-induced apoptosis (33, 34).

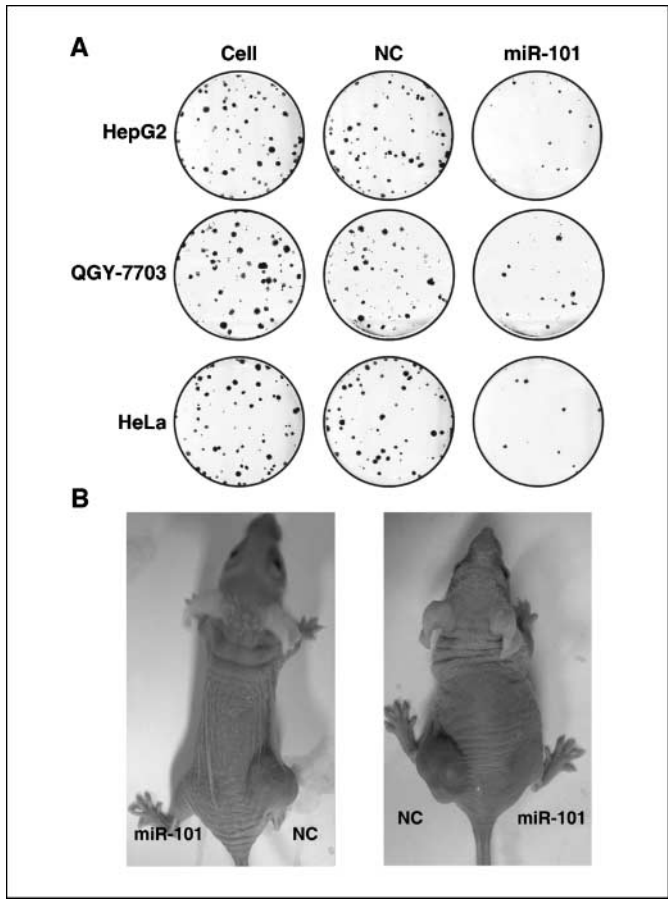

Figure 2. The effect of miR-101 on tumor cell growth *in vitro* and *in vivo*. *A,* effect of miR-101 on colony formation of cancer cell lines. Representative results of colony formation of nontransfected (*column 1*), NC-transfected (*column 2*), and miR-101–transfected (*column 3*) HepG2, QGY-7703, and HeLa cells. The results were reproducible in three independent experiments. *B,* effect of miR-101 on tumor formation in nude mouse xenograft model. NC- and miR-101–transfected HepG2 cells (1×10^5) were injected s.c. into either posterior flank of the same nude mice, respectively (as indicated). Photographs illustrate representative features of tumor growth 5 wk after inoculation.

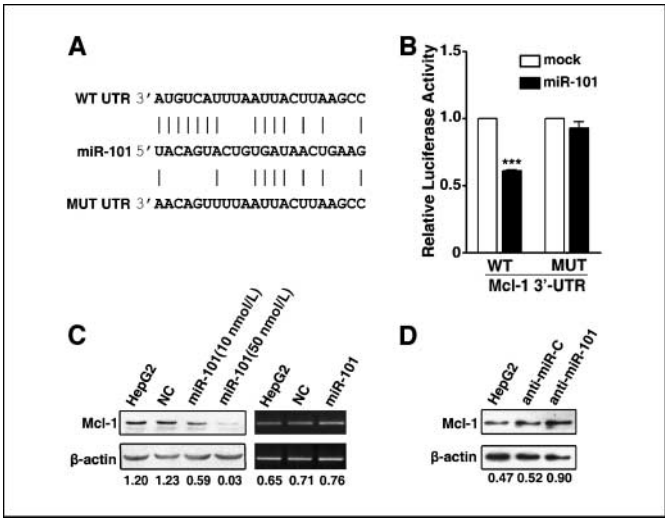

Figure 3. Mcl-1 is a direct target of miR-101. *A,* putative miR-101–binding sequence in the 3′-UTR of Mcl-1 mRNA. Mutation was generated on the Mcl-1 3′-UTR sequence in the complementary site for the seed region of miR-101, as indicated. A human Mcl-1 3′-UTR fragment containing wild-type or mutant miR-101–binding sequence was cloned downstream of the luciferase reporter gene. *B,* analysis of luciferase activity. Cells were cotransfected with *Renilla* luciferase expression construct pRL-TK, firefly luciferase reporter plasmid containing either wild-type or mutant Mcl-1 3′-UTR (indicated as WT or MUT on the *X*-axis), and either the miR-101–expressing plasmid (indicated as miR-101) or empty pcDNA3.0 (mock) vector. Luciferase activity was assayed 48 h after transfection. Firefly luciferase activity of each sample was normalized by *Renilla* luciferase activity. The normalized luciferase activity for the mock cells was set as relative luciferase activity 1. Columns, mean of at least three independent experiments done in duplicate; *bars,* SEM. ***, $P < 0.001$, compared with cells transfected with empty pCDNA3.0 vector. *C,* suppressed expression of endogenous Mcl-1 by miR-101. Western blot (*left*) and reverse transcription-PCR (*right*) were used to monitor the expression level of endogenous Mcl-1 in HepG2 cells 48 h after transfection with miR-101 or control RNA duplex (NC). *D,* elevated expression of endogenous Mcl-1 by antagonism of miR-101. HepG2 cells were transfected with anti–miR-101 (inhibitor of miR-101) or anti–miR-C (negative control), and applied to Western blot analysis 48 h later. In *C* and *D,* β-actin was used as an internal control. The intensity for each band was densitometrically quantified. The value under each lane indicates the relative expression level of Mcl-1, which is represented by the intensity ratio between Mcl-1 and β-actin fragments in each lane. RNA oligoribonucleotides transfected into HepG2 cells are indicated over each lane. *HepG2,* nontransfected cells.

To validate whether Mcl-1 is a bona fide target of miR-101, a human Mcl-1 3′-UTR fragment containing wild-type or mutant miR-101–binding sequence (Fig. 3*A*) was cloned downstream of the firefly luciferase reporter gene. Interestingly, the relative luciferase activity of the reporter that contained wild-type 3′-UTR was significantly suppressed when pc3-miR-101 was cotransfected (Fig. 3*B*). In contrast, the luciferase activity of mutant reporter was unaffected by simultaneous transfection of pc3-miR-101 (Fig. 3*B*), indicating that miR-101 may suppress gene expression through miR-101–binding sequence at the 3′-UTR of Mcl-1.

The effect of miR-101 on the endogenous expression of Mcl-1 was further examined. We found that ectopic expression of miR-101 caused a dose-dependent decrease in Mcl-1 protein but not mRNA level (Fig. 3*C*). Moreover, inhibition of endogenous miR-101 by synthetic miR-101 inhibitor (anti–miR-101) resulted in up-regulation of the Mcl-1 protein (Fig. 3*D*). These data suggest that miR-101 may inhibit the expression of Mcl-1 at posttranscriptional level by directly targeting the 3′-UTR of Mcl-1 mRNA.

miR-101 sensitizes hepatoma cells to apoptosis. It is well demonstrated that knockdown of Mcl-1 can sensitize cancer cells to apoptosis induced by different stimuli, such as serum starvation (33) or chemotherapeutic drugs (34). Considering miR-101 as a negative regulator of Mcl-1, and evading apoptosis may favor malignant transformation or confer cancer cells with resistance to chemotherapeutic drugs, we further investigated whether miR-101 could promote apoptosis of tumor cells. We found that miR-101 had no obvious effect on cell viability under normal culture conditions (data not shown).

Rapid growth of malignancy results in insufficient blood supply; solid cancer cells thus should evolve to tolerate nutrition starvation. The effect of miR-101 on the apoptosis of serum-deprived HepG2 cells was hereby evaluated by morphologic examination, cell viability, and caspase-3/7 activity assays. Twenty-four hours after transfection with NC or miR-101, cells were deprived of serum for 48 or 72 h before morphologic examination. Compared with NC-transfected cells, miR-101 transfectants displayed higher apoptotic rates both 48 h (31.2% versus 16.5%) and 72 h (87.7% versus 35.1%) after serum starvation (Fig. 4*A*), whereas NC transfectants revealed a similar frequency of apoptosis as nontransfected HepG2 cells (Fig. 4*A*). The cell viability analysis

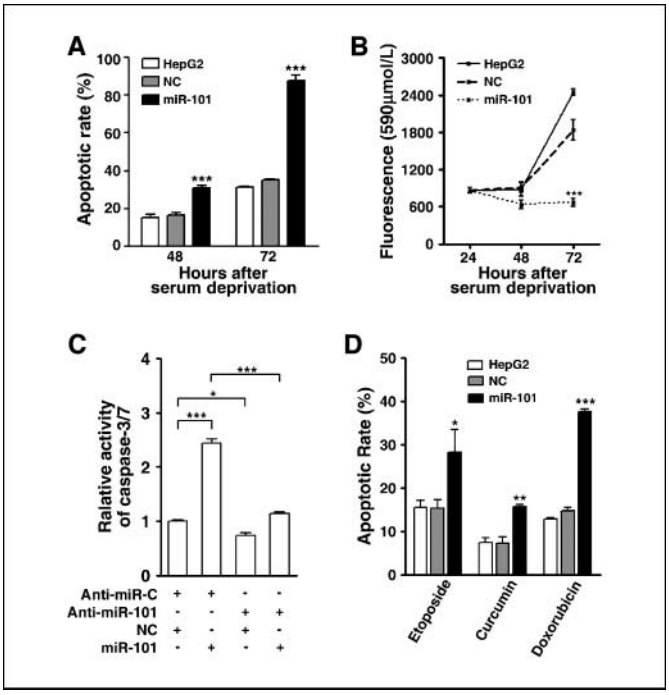

Figure 4. miR-101 sensitizes cancer cells to apoptosis. *A* to *C,* miR-101 sensitizes cancer cells to serum starvation–induced apoptosis. HepG2 cells were reverse transfected with RNA oligoribonucleotides (as indicated) and cultured in DMEM containing 10% FBS for 24 h. Then, the medium was replaced with serum-free DMEM for the indicated times and cells were applied to apoptosis analysis. Nontransfected cells (HepG2) were also included as control. In *A*, examination for apoptotic morphology was performed 48 and 72 h after serum starvation by staining cells with DAPI. In *B*, cell viability was evaluated by Alamar blue assay 24, 48, and 72 h after serum deprivation. In *C,* the relative caspase-3/7 activity was measured using caspase-Glo 3/7 assay 48 h after serum starvation. The caspase-3/7 activity for cells transfected with the controls (*column 1*) was set as relative caspase-3/7 activity 1. *D,* miR-101 sensitizes cancer cells to chemotherapeutic drug-induced apoptosis. HepG2 cells were reverse transfected with RNA duplex (as indicated) for 24 h, refreshed with medium containing etoposide (1.5 μg/mL for 48 h), curcumin (12.5 μmol/L for 48 h), or doxorubicin (0.2 μg/mL for 36 h), followed by apoptosis analysis using DAPI staining. Nontransfected cells (HepG2) were also included as control. *Columns,* mean of at least three independent experiments; *bars,* SEM. *, $P < 0.05$; **, $P < 0.01$; ***, $P < 0.001$, compared with NC-transfected and nontransfected cells or comparison between two groups as indicated.

using Alamar blue (Fig. 4*B*) also showed that miR-101 was effective in suppressing the growth of HepG2 cells under serum starvation. Furthermore, obvious increase in caspase-3/7 activity was found in miR-101–transfected cells compared with NC transfectants (~2.4-fold; Fig. 4*C, columns 1* and *2*). Interestingly, antagonism with anti–miR-101 counteracted the apoptosis-promoting effects of both exogenous (Fig. 4*C, columns 2* and *4*) and endogenous miR-101 (Fig. 4*C, columns 1* and *3*), although the extent of antagonism was more evident on the exogenous than the endogenous miR-101, which might be explained by the low basal level of miR-101 in HepG2 cells (Fig. 1*A, lane 4*). Taken together, these results indicate that miR-101 increases the sensitivity of cancer cells to serum starvation.

Next, we investigated whether miR-101 could sensitize tumor cells to chemotherapeutic drug–induced apoptosis. Compared with the NC-transfected group, enhanced expression of miR-101 caused obvious increase in the apoptotic rates of HepG2 cells exposed to etoposide, curcumin, or doxorubicin (1.8-, 2.2-, and 2.6-fold, respectively; Fig. 4*D*). These data clearly suggest a role of miR-101 in sensitizing cancer cells to chemotherapeutic drugs.

Mcl-1 is potentially involved in miR-101–regulated apoptosis. To investigate whether Mcl-1 is involved in miR-101–promoted apoptosis, the effect of miR-101 on the Mcl-1 expression under the condition of serum starvation was first examined. The repression effect of miR-101 was still observed (Supplementary Fig. S3). We then investigated whether reduction of Mcl-1 expression may mimic the apoptosis-promoting effect of miR-101 overexpression. HepG2 was transfected with siMCL1 or NC for 24 h and then applied to serum starvation for another 48 h. The results revealed that siMCL1 transfection caused significant reduction in the levels of Mcl-1 mRNA and protein (Fig. 5*A*). Furthermore, siMCL1 transfectants displayed obvious increases both in the capase-3/7 activity (1.7-fold; Fig. 5*B*) and in the proportion of cells with apoptotic morphology (2.3-fold; Fig. 5*C*), compared with NC-transfected cells. Notably, the apoptosis-promoting effect of Mcl-1 knockdown was similar to that of miR-101 overexpression (Fig. 5*B* and *C*). These results were reproducible with other two hepatoma cell lines, QGY-7703 and SMMC-7721 (Fig. 5*C*). Next, we examined whether Mcl-1 could counteract the proapoptotic function of miR-101. HepG2 cells were transfected with miR-101 duplex for 24 hours and followed by transfection with pc3-gab-MCL1, which encoded the entire *Mcl-1* coding sequence but lacked the 3′-UTR of Mcl-1 mRNA. Interestingly, the resulting Mcl-1 overexpression obviously abrogated miR-101–promoted apoptosis (Fig. 5*D*). Taken together, our results suggest that Mcl-1 is potentially involved in miR-101–regulated apoptosis.

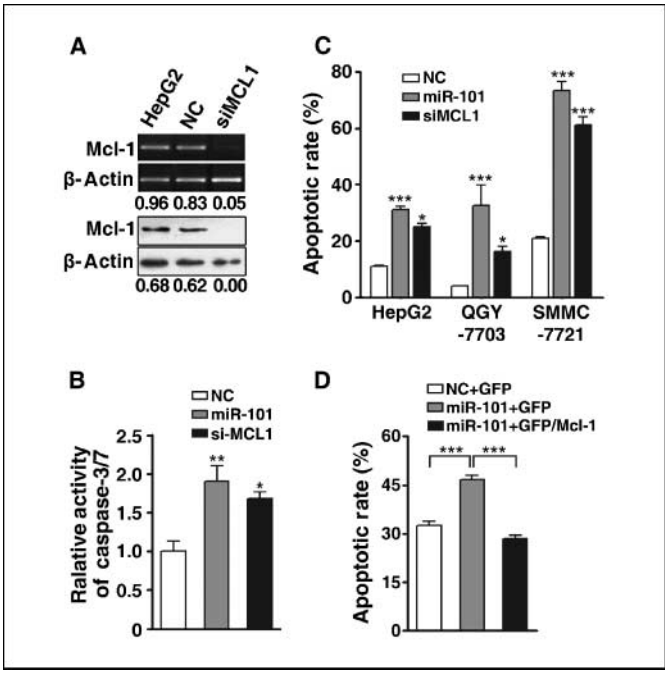

Figure 5. Mcl-1 is involved in miR-101–promoted apoptosis. *A,* siMCL1 efficiently inhibits the expression of Mcl-1 at both mRNA and protein levels. RT-PCR (*top*) and Western blot (*bottom*) were used to monitor the expression of endogenous Mcl-1 48 h after transfection with siRNA for MCL1 (siMCL1) or control RNA (NC). Nontransfected cells (HepG2) were also included as control. β-Actin served as an internal control. The intensity for each band was densitometrically quantified. The value under each lane indicates the relative expression level of Mcl-1, which is represented by the intensity ratio between the Mcl-1 and the β-actin fragments in each lane. *B* and *C,* either Mcl-1 knockdown or miR-101 overexpression increases the cellular sensitivity to apoptosis. In *B,* HepG2 cells were reverse transfected with siMCL1, miR-101, or control RNA (NC) for 24 h, followed by serum deprivation for 48 h. Cells were then applied to the assay for caspase-3/7 activity. The caspase-3/7 activity for cells transfected with NC (*column 1*) was set as relative caspase-3/7 activity 1. In *C,* cells (indicated on the *X*-axis) were transfected with siMCL1, miR-101, or NC for 24 h, followed by serum deprivation for 48 h (HepG2) or 72 h (QGY-7703 and SMMC-7721). Examination for apoptotic morphology was performed by staining cells with DAPI. *D,* overexpression of Mcl-1 abrogates the proapoptotic effect of miR-101. HepG2 cells were first transfected with miR-101 or NC duplex, and then with Mcl-1–expressing vector pc3-gab-MCL1 (indicated as GFP/Mcl-1) or empty vector pc3-gab (GFP) 24 h later. Twenty-four hours after vector transfection, cells were serum deprived for another 24 h before morphologic examination for apoptotic cells. *Columns,* mean of at least three independent experiments; *bars,* SEM. *, $P < 0.05$; **, $P < 0.01$; ***, $P < 0.001$, compared with NC-transfected cells or comparison between two groups as indicated.

Discussion

Although deregulation of miRNAs has been frequently observed in tumor tissues (3, 4), little is known about the molecular mechanisms by which miRNAs modulate the process of tumorigenesis and the behavior of cancer cells. We showed that miR-101 was frequently down-regulated in both hepatoma cell lines and human HCC tissues. We also revealed that miR-101 could suppress colony formation *in vitro*, inhibit tumor growth *in vivo*, and sensitize hepatoma cell lines to apoptosis induced by serum starvation as well as chemotherapeutic drugs. We further characterized Mcl-1 as a functional target of miR-101. Reduced expression of miR-101 has been observed in different types of cancers (5, 27–30). In addition, reduced expression of miR-101 is associated with worse survival of HCC patients (17). All these findings emphasize a fundamental role of miR-101 in tumorigenesis, especially in the development of HCC.

Apoptosis is a major barrier that must be circumvented during malignant transformation. Cancer cells evolve to evade apoptosis so that they can escape from being cleared away by the surveillance system and can survive in the crucial tumor microenvironment, such as hypoxia and low nutrition (35). In this study, we showed that miR-101 sensitized cancer cells to serum deprivation–induced apoptosis, whereas the inhibitor of miR-101 antagonized this effect of miR-101, suggesting that miR-101 may play a critical role in the adaptation of cancer cells to low nutrition. Growing numbers of miRNAs have been implicated in the regulation of apoptotic cell death and in the development of cancers. For instance, miR-15a and miR-16-1, which are down-regulated in the majority of chronic

lymphocytic leukemia patients, induce apoptosis by down-regulating Bcl-2 (7). On the other hand, miRNAs acting in an antiapoptotic manner can be illustrated by miR-21, which is frequently overexpressed in cancers (8, 9).

Mcl-1 is an antiapoptotic member of Bcl-2 family. Depletion of Mcl-1 has been well proven to sensitize human cancer cells to apoptosis (32–34). Furthermore, the *Mcl-1* transgenic mice exhibit a high probability of developing B-cell lymphoma (36). Although *Mcl-1* mutation is an infrequent event, increased Mcl-1 protein level is commonly observed in various types of cancers, including HCC (32). Even more, overexpression of Mcl-1 is correlated with shorter survival of cancer patients (37), which is consistent with the finding that down-regulation of miR-101 is associated with worse survival (17). We postulate that functional loss of miR-101 may result in enhanced expression of Mcl-1 and in turn the resistance of cells to apoptosis, which consequently favors tumor progression.

To date, three genes, including *cyclooxygenase-2* (*COX-2/PTGS2*), *EZH2/ENX-1*, and *MYCN*, have been identified as targets of miR-101 (38, 39). miR-101 has been implicated in the process of mouse embryo implantation by targeting *COX-2* (38). It has been shown that COX-2 signaling is involved in hepatocarcinogenesis and COX-2 inhibitors prevent HCC cell growth *in vitro* and in animal models (40). *EZH2/ENX-1* and *MYCN* are another two targets of miR-101 confirmed by the luciferase reporter system (39). EZH2 has been shown to be overexpressed in HCC, and suppression of EZH2 in hepatoma cell lines significantly reduced their growth rate *in vitro* and markedly diminished their tumorigenicity *in vivo* (41). *MYCN* is a member of *MYC* family. Amplification of this gene has been observed in a variety of tumors, most notably neuroblastomas (42). The target genes regulated by miR-101 may function spatiotemporally or in cooperation in different cellular processes. Our identification of Mcl-1 as a target of miR-101 provides new insights into the mechanisms underlying tumorigenesis and resistance to apoptosis. It is fantastic that a miRNA controls a number of genes that favor the process of tumorigenesis, as introduction of such a single miRNA may modulate complex downstream signals and even prevent malignant transformation.

It is noteworthy that miR-101 is significantly down-regulated in the majority of cancer cell lines and cancer tissues examined, and miR-101 not only suppresses colony formation *in vitro* and tumorigenicity *in vivo* but also sensitizes cancer cells to apoptosis induced by various chemotherapeutic drugs. Therefore, therapeutic strategies to introduce miR-101 into cancer cells may be potentially useful not only in retarding the process of tumorigenesis but also in sensitizing cancer cells to anticancer therapy. Further work is warranted to evaluate the application of miR-101 in cancer therapy *in vivo*. Moreover, miR-101 may also be used as a prognostic factor for cancer patients.

The microarray analysis in this study identified 29 miRNAs that were significantly differentially expressed in HCC tissues. Compared with previous studies in HCC, we found similar trend of deregulation in 11 miRNAs, including miR-101 (5), miR-125b (8), miR-195 (13, 14, 16), miR-199a (5, 13–15), miR-216a (18), miR-210 (8), miR-222 (8, 15, 16, 18), miR-224 (13, 15, 18), miR-223 (5, 14), miR-25 (18), and miR-29c (43). On the other hand, there also exists inconsistency among others and our results, which may attribute to different methodologies used, and/or distinct etiologic factors in different studied cohorts, such as HBV, HCV, and aflatoxin B1 exposure. The majority of HCC patients included in this study were HBsAg positive. Therefore, the miRNA expression patterns we identified may mainly represent the alterations in HBV-positive HCC tissues. Because only one HBV-negative sample in each of the HCC and normal control groups is used in our microarray analysis, we were unable to perform statistical comparison on the profiles of differentially expressed miRNAs between HBV-positive and HBV-negative HCCs. Obviously, future studies including larger size of HBV-positive and HBV-negative samples are required to elucidate the effect of HBV infection on the outcome of miRNA profiles in HCC.

It is unlikely that HBV infection itself but not the tumorigenesis induced the differential expression patterns of miRNAs in our set of HCCs. This contention is based on the following observations. First, HBV infection was prevalent in both HCC and normal control groups used in microarray analysis, with two of three normal liver tissues and four of five HCC samples were HbsAg positive. Second, the expression analysis disclosed that miR-101 was down-regulated in 94.1% of tumor samples (Fig. 1*B*), compared with matched adjacent noncancerous tissues. Furthermore, HBV-negative HCC tissue (no. 714 in Fig. 1*B*) displayed ~90% reduction in the miR-101 level, relative to the corresponding nontumor sample. Third, it has been reported that HBV infection alone is insufficient to induce major changes in miRNA expression (5).

In summary, we report the altered miRNA expression pattern in HCC and investigate the potential role of miR-101 in tumorigenesis. Our data suggest an important role of miR-101 in the molecular etiology of cancer and implicate the potential application of miR-101 in cancer therapy.

Disclosure of Potential Conflicts of Interest

No potential conflicts of interest were disclosed.

Acknowledgments

Received 7/28/2008; revised 10/6/2008; accepted 11/6/2008.

Grant support: Ministry of Science and Technology of China (2005CB724600, 2007AA02Z124), Ministry of Education of China (IRT0447), and the Natural Science Foundation of Guangdong Province (NSF-05200303).

The costs of publication of this article were defrayed in part by the payment of page charges. This article must therefore be hereby marked *advertisement* in accordance with 18 U.S.C. Section 1734 solely to indicate this fact.

References

1. Bartel DP. MicroRNAs: genomics, biogenesis, mechanism, and function. Cell 2004;116:281–97.
2. Calin GA, Sevignani C, Dumitru CD, et al. Human microRNA genes are frequently located at fragile sites and genomic regions involved in cancers. Proc Natl Acad Sci U S A 2004;101:2999–3004.
3. Lu J, Getz G, Miska EA, et al. MicroRNA expression profiles classify human cancers. Nature 2005;435:834–8.
4. Volinia S, Calin GA, Liu CG, et al. A microRNA expression signature of human solid tumors defines cancer gene targets. Proc Natl Acad Sci U S A 2006;103:2257–61.
5. Jiang J, Gusev Y, Aderca I, et al. Association of microRNA expression in hepatocellular carcinomas with hepatitis infection, cirrhosis, and patient survival. Clin Cancer Res 2008;14:419–27.
6. Calin GA, Ferracin M, Cimmino A, et al. A microRNA signature associated with prognosis and progression in chronic lymphocytic leukemia. N Engl J Med 2005;353:1793–801.
7. Cimmino A, Calin GA, Fabbri M, et al. miR-15 and miR-16 induce apoptosis by targeting BCL2. Proc Natl Acad Sci U S A 2005;102:13944–9.
8. Meng F, Henson R, Wehbe-Janek H, Ghoshal K, Jacob ST, Patel T. MicroRNA-21 regulates expression of the PTEN tumor suppressor gene in human hepatocellular cancer. Gastroenterology 2007;133:647–58.

9. Asangani IA, Rasheed SA, Nikolova DA, et al. MicroRNA-21 (miR-21) post-transcriptionally downregulates tumor suppressor Pdcd4 and stimulates invasion, intravasation and metastasis in colorectal cancer. Oncogene 2008;27:2128–36.

10. Parkin DM, Bray F, Ferlay J, Pisani P. Global cancer statistics, 2002. CA Cancer J Clin 2005;55:74–108.

11. Su H, Zhao J, Xiong Y, et al. Large-scale analysis of the genetic and epigenetic alterations in hepatocellular carcinoma from Southeast China. Mutat Res 2008;641:27–35.

12. Farazi PA, DePinho RA. Hepatocellular carcinoma pathogenesis: from genes to environment. Nat Rev Cancer 2006;6:674–87.

13. Murakami Y, Yasuda T, Saigo K, et al. Comprehensive analysis of microRNA expression patterns in hepatocellular carcinoma and non-tumorous tissues. Oncogene 2006;25:2537–45.

14. Gramantieri L, Ferracin M, Fornari F, et al. Cyclin G1 is a target of miR-122a, a microRNA frequently downregulated in human hepatocellular carcinoma. Cancer Res 2007;67:6092–9.

15. Ladeiro Y, Couchy G, Balabaud C, et al. MicroRNA profiling in hepatocellular tumors is associated with clinical features and oncogene/tumor suppressor gene mutations. Hepatology 2008;47:1955–63.

16. Wong QW, Lung RR, Law PT, et al. MicroRNA-223 is commonly repressed in hepatocellular carcinoma and potentiates expression of Stathmin1. Gastroenterology 2008;135:257–69.

17. Budhu A, Jia HL, Forgues M, et al. Identification of metastasis-related microRNAs in hepatocellular carcinoma. Hepatology 2008;47:897–907.

18. Wang Y, Lee AT, Ma JZ, et al. Profiling microRNA expression in hepatocellular carcinoma reveals microRNA-224 up-regulation and apoptosis inhibitor-5 as a microRNA-224-specific target. J Biol Chem 2008;283:13205–15.

19. Fornari F, Gramantieri L, Ferracin M, et al. MiR-221 controls CDKN1C/p57 and CDKN1B/p27 expression in human hepatocellular carcinoma. Oncogene 2008;27:5651–61.

20. Bolstad BM, Irizarry RA, Astrand M, Speed TP. A comparison of normalization methods for high density oligonucleotide array data based on variance and bias. Bioinformatics 2003;19:185–93.

21. Park W, Li J, Song R, Messing J, Chen X. CARPEL FACTORY, a Dicer homolog, and HEN1, a novel protein, act in microRNA metabolism in *Arabidopsis thaliana*. Curr Biol 2002;12:1484–95.

22. Xu T, Zhu Y, Wei QK, et al. A functional polymorphism in the miR-146a gene is associated with the risk for hepatocellular carcinoma. Carcinogenesis 2008;29:2126–31.

23. Lim LP, Lau NC, Garrett-Engele P, et al. Microarray analysis shows that some microRNAs downregulate large numbers of target mRNAs. Nature 2005;433:769–73.

24. Ragnarsson G, Eiriksdottir G, Johannsdottir JT, Jonasson JG, Egilsson V, Ingvarsson S. Loss of heterozygosity at chromosome 1p in different solid human tumours: association with survival. Br J Cancer 1999;79:1468–74.

25. An HX, Claas A, Savelyeva L, et al. Two regions of deletion in 9p23-24 in sporadic breast cancer. Cancer Res 1999;59:3941–3.

26. Li SP, Wang HY, Li JQ, et al. Genome-wide analyses on loss of heterozygosity in hepatocellular carcinoma in Southern China. J Hepatol 2001;34:840–9.

27. Yanaihara N, Caplen N, Bowman E, et al. Unique microRNA molecular profiles in lung cancer diagnosis and prognosis. Cancer Cell 2006;9:189–98.

28. Iorio MV, Ferracin M, Liu CG, et al. MicroRNA gene expression deregulation in human breast cancer. Cancer Res 2005;65:7065–70.

29. Lui WO, Pourmand N, Patterson BK, Fire A. Patterns of known and novel small RNAs in human cervical cancer. Cancer Res 2007;67:6031–43.

30. Iorio MV, Visone R, Di Leva G, et al. MicroRNA signatures in human ovarian cancer. Cancer Res 2007;67:8699–707.

31. Derenne S, Monia B, Dean NM, et al. Antisense strategy shows that Mcl-1 rather than Bcl-2 or Bcl-x(L) is an essential survival protein of human myeloma cells. Blood 2002;100:194–9.

32. Sieghart W, Losert D, Strommer S, et al. Mcl-1 overexpression in hepatocellular carcinoma: a potential target for antisense therapy. J Hepatol 2006;44:151–7.

33. Austin M, Cook SJ. Increased expression of Mcl-1 is required for protection against serum starvation in phosphatase and tensin homologue on chromosome 10 null mouse embryonic fibroblasts, but repression of Bim is favored in human glioblastomas. J Biol Chem 2005;280:33280–8.

34. Schulze-Bergkamen H, Fleischer B, Schuchmann M, et al. Suppression of Mcl-1 via RNA interference sensitizes human hepatocellular carcinoma cells towards apoptosis induction. BMC Cancer 2006;6:232.

35. Hanahan D, Weinberg RA. The hallmarks of cancer. Cell 2000;100:57–70.

36. Zhou P, Levy NB, Xie H, et al. MCL1 transgenic mice exhibit a high incidence of B-cell lymphoma manifested as a spectrum of histologic subtypes. Blood 2001;97:3902–9.

37. Wuilleme-Toumi S, Robillard N, Gomez P, et al. Mcl-1 is overexpressed in multiple myeloma and associated with relapse and shorter survival. Leukemia 2005;19:1248–52.

38. Chakrabarty A, Tranguch S, Daikoku T, Jensen K, Furneaux H, Dey SK. MicroRNA regulation of cyclooxygenase-2 during embryo implantation. Proc Natl Acad Sci U S A 2007;104:15144–9.

39. Lewis BP, Shih IH, Jones-Rhoades MW, Bartel DP, Burge CB. Prediction of mammalian microRNA targets. Cell 2003;115:787–98.

40. Leng J, Han C, Demetris AJ, Michalopoulos GK, Wu T. Cyclooxygenase-2 promotes hepatocellular carcinoma cell growth through Akt activation: evidence for Akt inhibition in celecoxib-induced apoptosis. Hepatology 2003;38:756–68.

41. Chen Y, Lin MC, Yao H, et al. Lentivirus-mediated RNA interference targeting enhancer of zeste homolog 2 inhibits hepatocellular carcinoma growth through down-regulation of stathmin. Hepatology 2007;46:200–8.

42. Schwab M. Amplified MYCN in human neuroblastoma: paradigm for the translation of molecular genetics to clinical oncology. Ann N Y Acad Sci 2002;963:63–73.

43. Varnholt H, Drebber U, Schulze F, et al. MicroRNA gene expression profile of hepatitis C virus-associated hepatocellular carcinoma. Hepatology 2008;47:1223–32.